NIPPON STEEL TECHNICAL REPORT No. 93 January 2006

UDC 629 . 114 : 66 . 097 . 5 : 539 . 377

Elastic-plastic Thermal Stress Analysis of Metal Substrates for Catalytic Converters

Shogo KONYA*[1]

Abstract

In order to quantitatively evaluate mechanical durability of metal substrates for catalytic converters under heat cycles, thermal stresses and strains were simulated by FEM elastic-plastic analysis. Flat and corrugated sheets constituting honeycomb structures were directly modeled by thick-shell elements. It was reported that the asymmetric joint structure with the "Strengthened Outer Layer" could provide metal substrates with high mechanical durability. From the results of analysis in this study, it was shown that metal substrates with the above-mentioned joint structure had high durability because the location of cracks generated in the sheets and direction of their propagation were controlled.

1. Introduction

The demand for cleaner automotive exhaust gas is growing year by year. This is reflected in increasingly stricter regulations on exhaust gas, particularly in Japan, the U.S. and in Europe over the last years. Hazardous substances such as HC, CO and NO_x in the exhaust gas are purified by a catalytic converter installed in the exhaust system of an automobile. However, immediately after starting an engine, the temperature of the catalyst is too low to work properly and the hazardous substances are emitted to the environment without being treated. Therefore, it is necessary to rapidly activate the catalyst through a quick warm-up process, and for this end, the heat capacity of a catalytic converter is reduced or a converter is installed closer to the exhaust manifold where the temperature of the incoming gas is higher. What is more, the latest trend of automotive engine design is such that the combustion temperature under high-load operation is made higher to reduce fuel consumption.

The catalyst is coated to the surface of a metal or ceramic substrate of a honeycomb structure. A metal substrate is used mainly for a high-power engine because of its lower gas-flow resistance than that of a ceramic substrate. When close-coupled to an exhaust manifold, a catalytic converter is exposed to high temperatures under high-load operation, and this leads to high thermal loads on the substrate. For this reason, excellent heat resistance, especially high mechanical durability against heat cycles, is required for a metal substrate.

As seen in **Photo 1**, a metal substrate is structured typically in

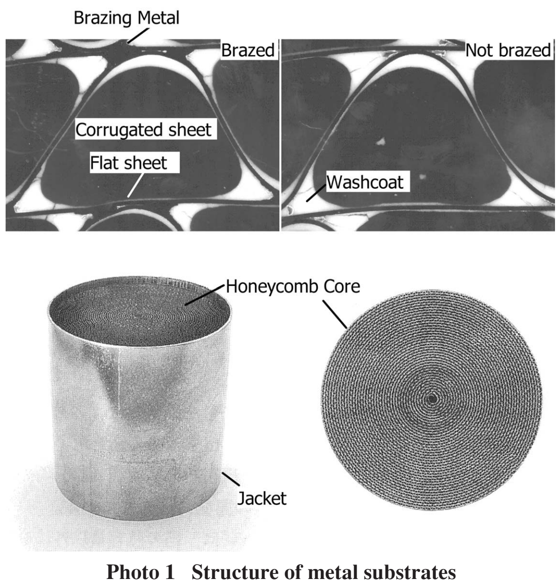

Photo 1 Structure of metal substrates

*[1] Advanced Technology Research Laboratories

the form of a honeycomb body consisting of cells having a triangular section formed by flat and corrugated stainless steel foils approximately 50 μm in thickness, and the honeycomb body is encased in a jacket. The thermal stress on the honeycomb body under heat loads is influenced significantly by the bonding structure of the flat and corrugated foils, and it is essential for obtaining good durability to optimize the bonding structure and control the thermal stress. In actual practice, in order to mitigate the thermal stress, the contact lines between the flat and corrugated foils are bonded only partially, and they are intentionally left without being bonded in some portions of the honeycomb body. This is the same with the contact between the honeycomb body and the jacket.

Takada et al. examined the durability of metal substrates of the three types of bonding structures shown in **Fig. 1** under heat cycles between 150 to 850℃ of exhaust gas temperature, and reported the results[1]. The dark areas in Fig. 1 represent the portions where the flat and corrugated foils were bonded to each other, and the white areas the portions where they were not.

In the structure shown in part (a) of Fig. 1, the flat and corrugated foils were not bonded in the center portion but were bonded in the whole round sections at the inlet and outlet ends of the honeycomb body, and the honeycomb body was bonded to the jacket at the center portion in the axial direction. In the structures shown in parts (b) and (c) of Fig. 1, the flat and corrugated foils were bonded to each other in some outermost laps across the whole length to form strengthened outer layers. In the structure of part (b), the foils were bonded also in the whole sections at the inlet and outlet ends of the honeycomb body, and the honeycomb body was bonded to the jacket at the center portion in the axial direction as in the structure of part (a). In the structure of part (c), on the other hand, the foils were bonded in the whole section only at the inlet end of the honeycomb body, and the honeycomb body was bonded to the jacket only at the outlet end, resulting in an asymmetric joint structure.

The honeycomb body of part (a) without the strengthened outer layers showed extremely poor durability: the flat foil broke at the outermost lap before completing 150 heat cycles, and the honeycomb body fatally failed, falling out of the jacket. In contrast, the honeycomb body of either of parts (b) and (c) with the strengthened outer layer showed much improved durability: it withstood 900 heat cycles without falling out of the jacket.

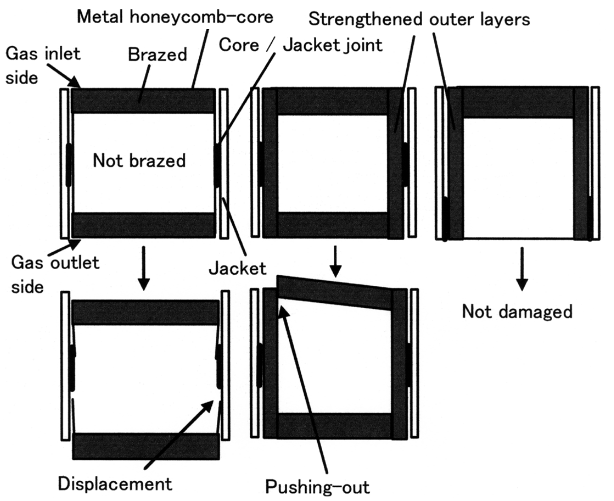

(a) Displacement before 150 cycles (b) No displacement after 900 cycles (c) No displacement after 900 cycles

Fig. 1 Effect of joint structures on mechanical durability of metal substrates (by Takada et al.[1])

Of the latter two bonding structures, that of part (b) where the foils were bonded in the whole sections at the inlet and outlet ends failed at the inlet portion and the honeycomb structure partially protruded (pushing-out) in the inlet direction as shown in the lower portion of part (b). In contrast, the pushing-out did not occur with the structure of part (c) where the foils were bonded in the whole section only in the inlet portion. These results showed that the asymmetric bonding structure having the strengthened outer layer was the most effective of the three in improving the durability of the metal substrate.

In quantitatively evaluating thermal stress on a metal substrate and adequately designing its structure, it is effective to analyze the thermal stress by methods such as the finite element method (FEM). An analysis method in which structural members are replaced with equivalent elements is applicable to the thermal stress analysis of a honeycomb body[2]. While such a method is effective in understanding the macroscopic deformation behavior of an entire honeycomb body, it does not give the stress and strain conditions of the foils that compose a honeycomb body.

In view of the above, instead of using equivalent elements, the flat and corrugated foils that composed a honeycomb body were directly represented with shell elements and the elastic-plastic thermal stress analysis of the honeycomb body by the FEM was performed. Then, using the test results of Takada et al.[1] on the relationship between the mechanical durability of honeycomb bodies and their bonding structure as model cases, an attempt was made to quantify the effects of the strengthened outer layers and asymmetric bonding structure on the mechanical durability of the honeycomb body. This paper reports on the analysis and its results.

2. Method of Analysis

2.1 Finite element model of honeycomb structure

MARC® was used for the elastic-plastic thermal stress analysis of metal substrates. The metal substrates for the analysis were formed by spirally winding a flat and a corrugated foil, each 30μm in thickness, alternately one on the other and encasing the honeycomb body thus formed in a jacket; its outer diameter was 80 mm including the thickness of the jacket of 1.5 mm and the height (axial length) was 100 mm. The corrugated foil had a wave height of 1.25 mm at a pitch of 2.5 mm, and thus the honeycomb body had 62 cells/cm^2 in section (400 cpsi).

Since it was inefficient to model an entire cylindrical honeycomb body, a periodical symmetric model having a sectorial section shape with an apex angle of 20° as shown in **Fig. 2** was used as the analysis model. All the 30 laps of the flat foil, 29 laps of the corrugated foil and jacket were modeled using bilinear thick-shell element with four nodes.

To minimize the number of the elements, while the foils were divided finely in the radial (r) and circumferential (θ) directions in which bending would be significant, they were divided more coarsely in the axial (z) direction in which the bending would be smaller, as shown in **Fig. 3**. It has to be noted, however, that the components were divided into comparatively smaller elements in the axial direction in the portions corresponding to the upper and lower ends of the joint between the jacket and the honeycomb body.

2.2 Bonding structures

The following three types of bonding structures shown in parts (a) to (c) of Fig. 1 were analyzed. These have also been reported by

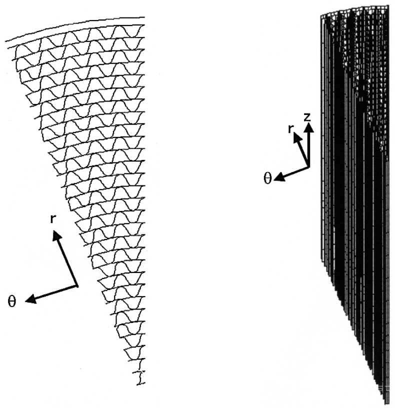

(a) Top view (b) Squint view

Fig. 2 Fan shaped periodical symmetric model of honeycomb structures

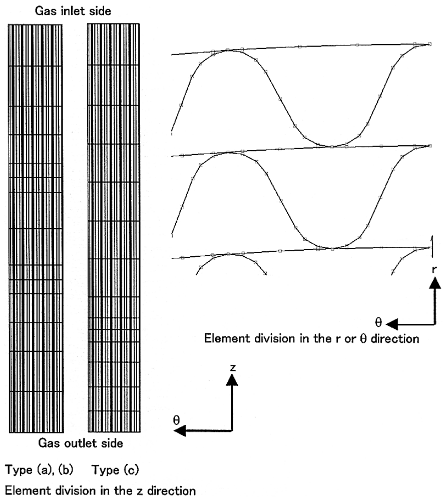

Fig. 3 FEM elements for thermal stress analysis

Takada et al.[1]:

(a) A bonding structure without the strengthened outer layer in which structure the flat and corrugated foils are bonded to each other in the whole round sections at the inlet and outlet ends of the honeycomb body to a depth of 20 mm. The flat foil of the honeycomb body is bonded to the jacket circumferentially through the outermost flat foil at the center of the axial length in a width of 25 mm. (This bonding structure is hereinafter referred to as Structure A.)

(b) A bonding structure in which the flat and corrugated foils are bonded to each other across the whole height (axial length) of the honeycomb body in three outermost layers (four laps of the flat foil and three laps of the corrugated foil) to form a strengthened outer layer. In addition, the foils are bonded to each other in the whole round sections at the inlet and outlet ends of the honeycomb body to a depth of 20 mm. The honeycomb body is bonded in the outermost flat foil to the jacket at the center of the axial length in a width of 25 mm. (This bonding structure is hereinafter referred to as Structure B.)

(c) A bonding structure in which the flat and corrugated foils are bonded to each other across the whole axial length of the honeycomb body in three outermost layers to form the strengthened outer layers. In addition, the foils are bonded to each other in the whole round section at the inlet end of the honeycomb body to a depth of 20 mm. The honeycomb body is bonded in the outermost flat foil to the jacket at the outlet end in a width of 25 mm, forming an asymmetric bonding structure. (This bonding structure is hereinafter referred to as Structure C.)

2.3 Models of bonded joints between flat and corrugated foils and that between honeycomb body and jacket

The metal substrate of a catalytic converter is bonded typically by brazing using a highly heat-resistant Ni-based filler metal. The thickness of the filler metal was not taken into consideration in the analysis, and the brazed joints were assumed to have the material properties of the foils or the jacket as the case might be.

Part (a) of **Fig. 4** shows a real joint between flat and corrugated foils, and part (b), the model of the joint used for the analysis. In the analysis, the width of a brazed joint was assumed to be approximately 370 μm, and thinking that the flat and corrugated sheets formed one unit at a joint, the thickness of the flat sheet was doubled in the bonded portion, with corrugated sheets fixed at both the ends of the double-thickness portion. The relative displacement and rotation of the flat and corrugated sheets at the nodes between them were totally restricted.

2.4 Models of non-bonded contact between flat and corrugated foils and that between honeycomb body and jacket

The contact between the flat and corrugated sheets along a non-bonded contact line was judged supposing that a non-linear spring was inserted between a node at a wave peak of the corrugated sheet and a node of the adjacent flat sheet. A spring constant was considered only in the radial direction; it was assumed to be zero with respect to the displacements in the circumferential and axial directions. The contact between the outermost lap of the flat sheet and the jacket where they were not bonded was judged in the same manner. Note that the friction between contact surfaces was not taken into consideration.

2.5 Other boundary conditions

With respect to the nodes on the r-z planes on both the sides of the periodical symmetric model shown in Fig. 2, the displacement in the θ direction and the rotation around the r and z axes were restricted. The displacement in the z direction of the nodes of the jacket corresponding to the inlet end was also restricted.

2.6 Material properties

The material properties in the temperature range of the analysis, namely the thermal expansion coefficient, Young's modulus and yield strength, of the jacket used in our analysis were the experimental

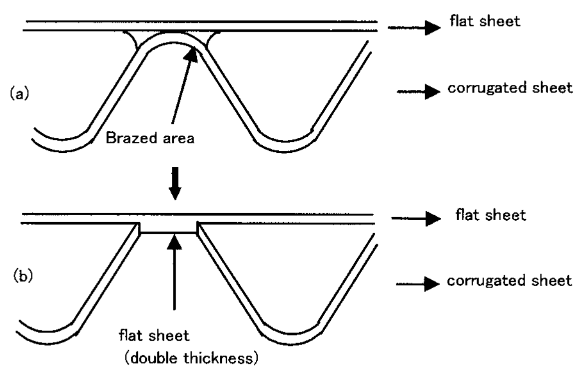

Fig. 4 Schematic diagram of model for brazing areas (a) Shape of the brazing area, (b) Concept for modeling brazing areas

data of SUS 430, and the same of the foils were those of a stainless steel of a Fe-20Cr-5Al system (YUS 205M1) that is commonly used for the metal substrate of a catalytic converter. The yield criterion of von Mises was used as yield condition.

2.7 Temperature distribution

The temperature distribution within a metal substrate was defined based on the experimental results of temperature measurement at durability test on an engine bench. A heat cycle at the durability test using an engine is 1,300 s long in total, consisting of a heating period of 480 s and a cooling period of 820 s. The heating period comprises an idling time of 30 s after starting the engine, a rotation rate increase to 6,000 rpm in 60 s and a constant- rotation rate at 6,000 rpm of 390 s, and the cooling period comprises a rotation rate decrease from 6,000 rpm to idling in 60 s, an idling time of 30 s and a holding time of 730 s with the engine stopping.

The temperature was measured at three points in the axial direction and six points in the radial direction. Based on the temperature distribution thus measured, the temperatures obtained from time to time were given to corresponding nodes, and the temperatures of the portions not corresponding to the measurement points were calculated through linear interpolation. The temperatures of all the nodes at the start of the first heat cycle were assumed to be 20℃, and those at the start of the second cycles were assumed to be the temperatures at the end of the preceding cooling period.

Fig. 5 shows the temperature change of the jacket and the outermost and 5th laps from the periphery and the center of the honeycomb body at a depth of 10 mm from the inlet end as a function of time. **Figs. 6 and 7** show the temperature distributions inside the honeycomb body in the radial direction at a depth of 10 mm from each of the inlet and outlet ends, respectively, at the time of the heating period when the temperature difference between the jacket and the center became largest (84 s), the end of the heating period (480 s), the end of the idling of the cooling period (570 s) and the end of the cooling period (1,300 s). The characteristics of the temperature distribution were as follows:

(1) In the radial direction, the temperature was low in the peripheral portion and high in the center during the heating period. The temperature gradient was steep especially in the outer five layers. The temperature difference between the jacket and the center was largest at approximately 84 s after the commencement of the heating period, and the temperature gradient decreased thereafter. The temperature was higher in the inlet-end portion than in the outlet-end portion.

(2) Just before the commencement of the cooling period (approximately 480 s), the temperature at the center of the inlet end rose to as high as approximately 950℃ despite the fact that the temperature of the incoming gas was approximately 880 ℃. The temperature at the center of the inlet end is an actually measured value and due to the exothermic reaction on the catalyst. The temperature difference in the axial direction became substantially nil at this time.

(3) For 90 s after the commencement of the cooling period, the reactor was cooled internally, especially at the inlet end, owing to the engine being idling. At this time, the temperature was lower at the center than at the peripheral portion especially in the inlet-end portion. Thereafter, the temperature distribution in the radial direction resumed the center-high pattern owing to external cooling because of the engine being stopping. The temperature increase just after engine stop, as seen in Fig. 5, is due to the cooling state change from internal to external.

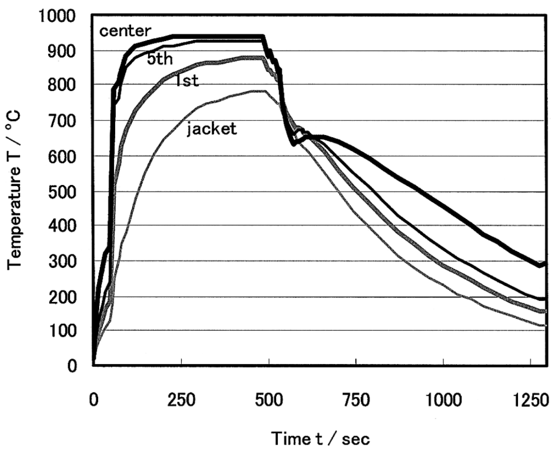

Fig. 5 Temperature history at the gas inlet side

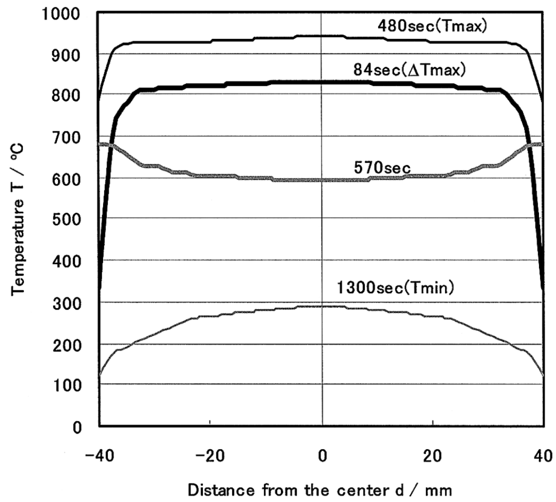

Fig. 6 Temperature distribution in the r direction at the gas inlet side

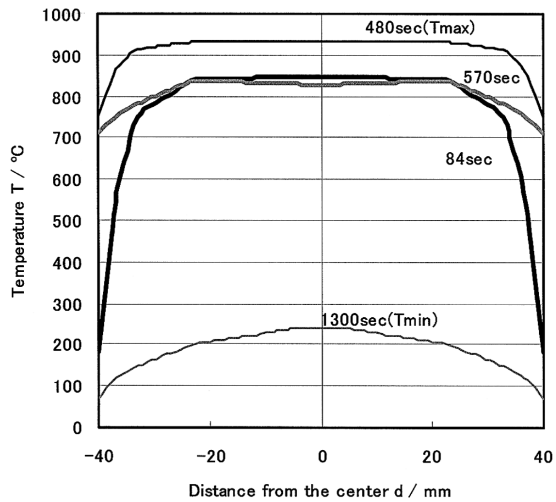

Fig. 7 Temperature distribution in the r direction at the gas outlet side

3. Results of Analysis

3.1 Effects of strengthened outer layers

According to the report of Takada et al., whereas with the bonding structure of part (a) of Fig. 1 (corresponding to Structure A) the honeycomb body was displaced from the jacket after a small number of heat cycles at the durability test using an engine, such a fatal failure did not occur with either of the bonding structures shown in parts (b) and (c) of Fig. 1 having the strengthened outer layers (corresponding to Structures B and C).

A similar durability test was conducted using an engine to inspect the catalyst substrates after the test. As a result, it was found that any fatal displacement of the honeycomb body as shown in part (a) of Fig. 1 did not occur with either of Structures B and C, but cracks developed in these structures in the flat foil in the outermost lap and the corrugated foil in the adjacent lap in the regions corresponding to the inlet- and outlet-side ends of the joint between the jacket and the honeycomb body, and the cracks propagated to a certain extent in the corrugated foil in the axial direction, as schematically illustrated in **Fig. 8**.

Figs. 9 and 10 show the change in the equivalent plastic strain in the outermost flat foil and that in the corrugated foil in the adjacent lap, respectively, that generated during two heat cycles in the portion near the inlet-side end of the joint between the jacket and the honeycomb body of each of the three bonding structures. The portion corresponds to that where the honeycomb body fractured or cracks developed in the foils.

Although the durability of Structure A was the lowest at the durability test with an engine, Figs. 9 and 10 show that the equivalent plastic strain was lowest in Structure A. However, in Structure A without the strengthened outer layers, the honeycomb structure is bonded to the jacket only through the outermost lap of the flat foil only 30μ m in thickness, and for this reason, when the flat foil breaks in all the outermost lap, the honeycomb body is severed from the jacket because the flat foil is not bonded to the adjacent corrugated foil, and the honeycomb body falls fatally out of the jacket even though the equivalent plastic strain is low.

In the case of Structure B or C with the strengthened outer layers, on the other hand, the equivalent plastic strain is significant in the portions at the ends of the joint between the jacket and honeycomb body, and initial cracks are likely to occur easily in the portions. **Fig. 11** shows the equivalent plastic strain generated in the flat foil at different positions in the axial direction in Structure C. The equivalent plastic strain is higher at positions 1 and 3 near the ends of the joint between the jacket and honeycomb body than that at position 2 away from the ends of the joint, indicating the likelihood of cracking at positions 1 and 3.

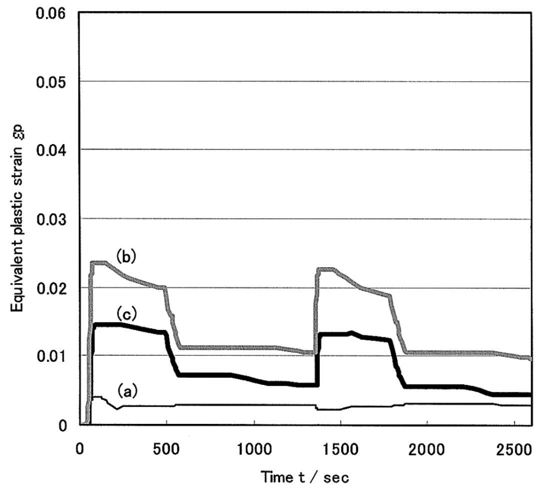

Fig. 9 Equivalent plastic strain in the outermost flat sheet

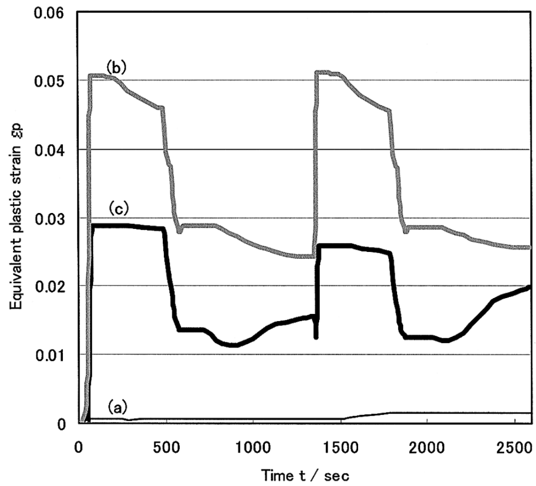

Fig. 10 Equivalent plastic strain in the outermost corrugated sheet

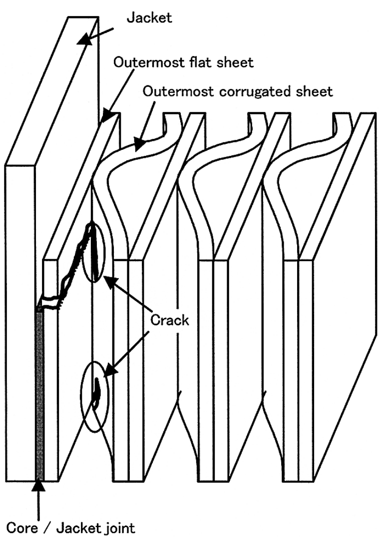

Fig. 8 Schematic diagram of the cracks generated in the substrate shown in the Fig. 1 (c)

Figs. 12 and 13 show the circumferential and axial components (σ_θ and σ_z) of the normal stress in the outermost corrugated foil at an end of the joint between the jacket and the honeycomb body in Structure C, expressed as functions of time. Fig. 12 shows the stress on the inner surface of the foil, and Fig. 13 that on the outer surface. The sign of σ_θ is inversed at the inner and outer surfaces, indicating that bending occurred. The absolute value of σ_θ is larger than that of σ_z; this means that the stress to propagate cracks in the axial direction was predominant. These analysis results explain the test result that cracks started at the ends of the joint between the jacket and the honeycomb body and propagated in the axial direction.

The foregoing indicates that with Structure B or C having the strengthened outer layers, large plastic strain is generated in the outermost flat foil and the corrugated foil in the adjacent lap at the positions corresponding to the ends of the joint between the jacket and honeycomb body, and cracks start at these positions. The cracks propagate in the axial direction, but in the case where there are the strengthened outer layers, the fatal displacement of the honeycomb body out of the jacket does not occur, because for it to occur, the cracks must propagate across the axial distance of 25 mm, the width of the joint between the jacket and honeycomb body. Therefore, Structure B or C with the strengthened outer layers is more resistant than Structure A without them, and is more durable.

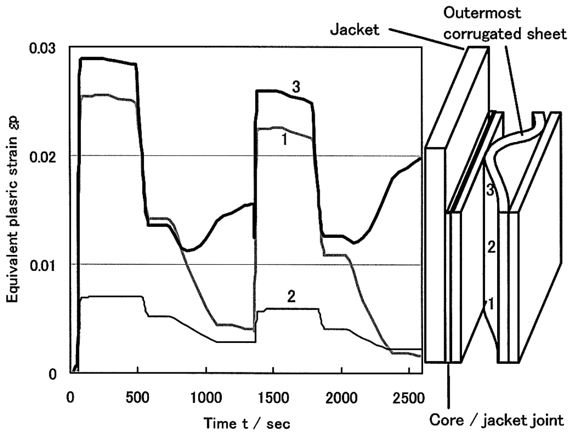

Fig. 11 Dependence of the position in the z direction on equivalent plastic strain in the outermost flat sheet of the substrate in the Fig. 1 (c)

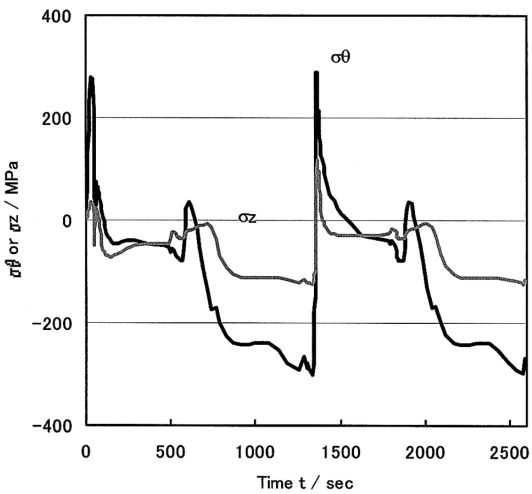

Fig. 12 σ_θ and σ_z in the inner surface in the outermost corrugated sheet

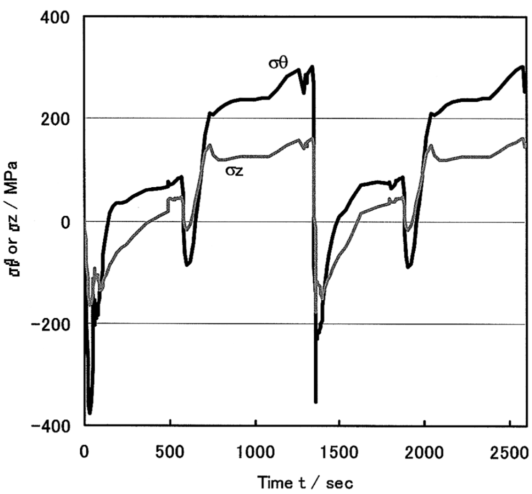

Fig. 13 σ_θ and σ_z in the outer surface in the outermost corrugated sheet

3.2 Effects of asymmetric bonding structure

Figs. 14 and 15 show the axial displacements of the flat foils of Structures B and C, respectively; the displacements were measured in each lap at the planes of the inlet and outlet ends at the time when the temperature difference within the honeycomb body was largest (84 s after the commencement of the heating period) at the durability test with an engine. Since the axial displacement of the jacket was restricted at the inlet end as a boundary condition, the displacement of the jacket at the inlet end was zero, and the displacement of the foil towards the inlet side is expressed as positive in the graphs, and that towards the outlet side as negative.

The coefficient of thermal expansion of the jacket material (SUS 430) was smaller than that of the foil material (Fe-20Cr-5Al), and the temperature of the jacket was lower than that of the honeycomb body, and as a consequence, the displacement of the honeycomb body was larger than that of the jacket. In addition, since the temperature of the honeycomb body was higher in the center portion than in the peripheral portion during the heating period, the displacement was

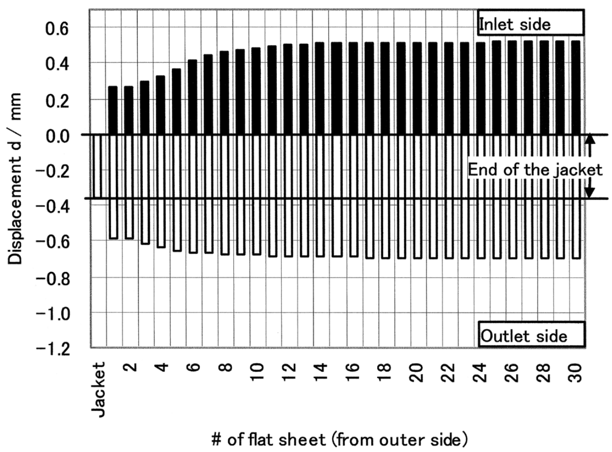

Fig. 14 Displacement of each flat sheet of the substrate in the Fig. 1 (b) in the z direction

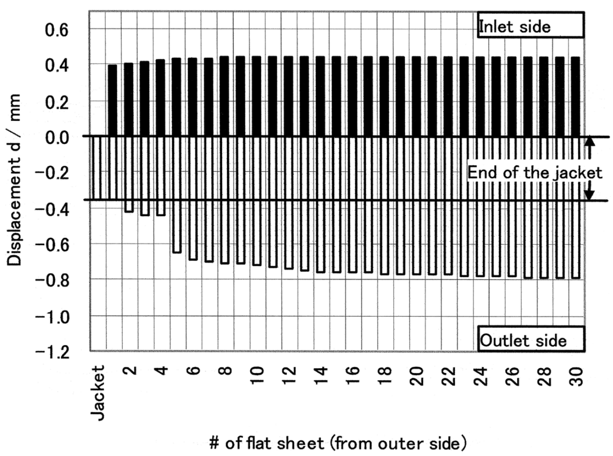

Fig. 15 Displacement of each flat sheet of the substrate in the Fig. 1 (c) in the z direction

larger in the center portion than in the peripheral portion.

With Structure B, the honeycomb body was bonded to the jacket at the center of its length and they were not bonded to each other at the inlet or outlet end, and for this reason, the displacement of the flat foil in the outermost lap during the heating period was larger than that of the jacket at both the inlet and outlet ends. With Structure C, in contrast, because the honeycomb body was bonded to the jacket at the outlet end, the displacements of the jacket and the flat foil in the outermost lap were the same at the outlet end.

With Structure B, in which the foils were bonded to each other at the inlet and outlet ends, the dependence of the foil displacement on radial position was larger at the inlet end than at the outlet. This is presumably because the temperature of the substrate was higher in the inlet side than in the outlet, therefore the yield point of the foil material was lower there, and as a result, the plastic deformation of the foils was larger in the inlet side. The difference in the displacement between adjacent laps was large especially between the 4th and 5th laps from the periphery, the position where the pushing-out occurred in the durability test with an engine, indicating that there was a large strain in that portion.

With Structure C, on the other hand, the displacement at the outlet end of the flat foil in the 1st to 4th laps from the periphery, corresponding to the strengthened outer layer, was significantly different from that in inner laps. This is because the foils were not bonded in the 5th and inner laps at the outlet end. It has to be noted, however, that the strain on the foils was small in the inner laps other than the strengthened outer layers even though the displacement was large, because their axial displacement was not restricted. The difference in the foil displacement in the radial direction at the inlet end was smaller in Structure C than in Structure B.

Fig. 16 compares Structures B and C in terms of the equivalent plastic strain in the 4th flat foil from the outer periphery at the inlet end near the joint between the flat and corrugated foils; here the strain is expressed as a function of time up to the end of the second heat cycle. Whereas plastic strain exceeding 2% repeated in Structure B, in which the foils were bonded to each other at both the inlet and outlet ends, indicating the occurrence of thermal fatigue, the level of plastic strain was lower in Structure C, in which the foils were not brazed at the outlet end. This analysis result agrees with the report of Takada et al. to the effect that pushing-out occurred with the bonding structure of part (b) of Fig. 1 (corresponding to Structure B), and it did not with the structure of part (c) (corresponding to Structure C).

As explained above, with Structure C of the asymmetric bonding structure, in which the foils are bonded to each other only at the inlet-end portion, the axial displacement of the foils at the outlet end is allowed because they are not restricted there, and the plastic strain that occurs near the foil joints in the inlet-end portion is reduced. This indicates that the asymmetric bonding structure in which the foils are bonded to each other only in one of the two ends is advantageous to improving the durability of the metal substrate for catalytic converters.

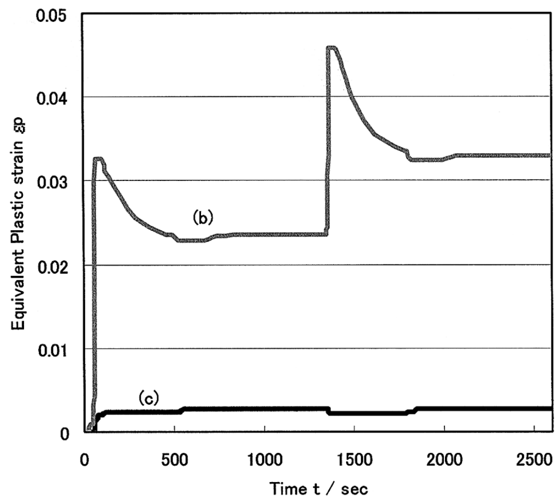

Fig. 16 Equivalent plastic strain in the 4th flat sheet at the gas inlet side surface

4. Conclusions

The elastic-plastic thermal stress on the metal substrate for a catalytic converter has been analyzed through direct modeling of the foils that compose the honeycomb body using shell elements. The analysis using the model has proved capable of explaining the pushing-out of a honeycomb body in which the foils are bonded to each other at both the inlet and outlet ends and the occurrence and propagation behavior of cracks of the foils in a honeycomb body that has strengthened outer layers.

The analysis has made it clear that a metal substrate of an asymmetric bonding structure with the strengthened outer layers, in particular, allows the axial expansion/contraction of the foils at the outlet end reducing the plastic strain imposed on the foils at the inlet-end portion and prevents the pushing-out of the honeycomb body, and that the cracking positions and propagation directions of foil cracks near the ends of the joint between the jacket and honeycomb body are controlled, and thus high durability is obtained with a substrate of this type of bonding structure.

In addition to the thermal stress, a metal substrate is subjected to external force such as vibration and the pressure of engine exhaust gas. A metal substrate having the strengthened outer layers is expected to be well resistant also to such external force.

References

1) Takada, T. et al.: SAE Paper. 910615. 1991
2) Reddy, K. P. et al.: SAE Paper. 940782. 1994